Research Article | Vol. 25, No. 2 | 23 Jan 2017 | OPTICS EXPRESS 681

Optics EXPRESS

Towards chip-scale optical frequency synthesis based on optical heterodyne phase-locked loop

SHAMSUL ARAFIN,[1,4] ARDA SIMSEK,[1] SEONG-KYUN KIM,[1] SARVAGYA DWIVEDI,[1] WEI LIANG,[2] DANNY ELIYAHU,[2] JONATHAN KLAMKIN,[1] ANDREY MATSKO,[2] LEIF JOHANSSON,[3] LUTE MALEKI,[2] MARK RODWELL,[1] AND LARRY COLDREN[1,5]

[1]*Department of Electrical and Computer Engineering, University of California at Santa Barbara, Santa Barbara, CA 93106, USA*
[2]*2OEwaves Inc., Pasadena, CA 91107, USA*
[3]*Freedom Photonics LLC, Santa Barbara, CA 93117, USA*
[4]*sarafin@ece.ucsb.edu*
[5]*coldren@ece.ucsb.edu*

Abstract: An integrated heterodyne optical phase-locked loop was designed and demonstrated with an indium phosphide based photonic integrated circuit and commercial off-the-shelf electronic components. As an input reference, a stable microresonator-based optical frequency comb with a 50-dB span of 25 nm (~3 THz) around 1550 nm, having a spacing of ~26 GHz, was used. A widely-tunable on-chip sampled-grating distributed-Bragg-reflector laser is offset locked across multiple comb lines. An arbitrary frequency synthesis between the comb lines is demonstrated by tuning the RF offset source, and better than 100Hz tuning resolution with ± 5 Hz accuracy is obtained. Frequency switching of the on-chip laser to a point more than two dozen comb lines away (~5.6 nm) and simultaneous locking to the corresponding nearest comb line is also achieved in a time ~200 ns. A low residual phase noise of the optical phase-locking system is successfully achieved, as experimentally verified by the value of –80 dBc/Hz at an offset of as low as 200 Hz.

OCIS codes: (250.5300) Photonic integrated circuits; (060.5625) Radio frequency photonics; (060.2840) Heterodyne; (140.0140) Lasers and laser optics; (140.3600) Lasers, tunable; (140.3945) Microcavities; (230.5750) Resonators

References and links

1. D. J. Jones, S. A. Diddams, J. K. Ranka, A. Stentz, R. S. Windeler, J. L. Hall, and S. T. Cundiff, "Carrier-envelope phase control of femtosecond mode-locked lasers and direct optical frequency synthesis," Science **288**(5466), 635–639 (2000).
2. J. Castillega, D. Livingston, A. Sanders, and D. Shiner, "Precise measurement of the J = 1 to J = 2 fine structure interval in the 2(3)P state of helium," Phys. Rev. Lett. **84**(19), 4321–4324 (2000).
3. M. J. Thorpe, K. D. Moll, R. J. Jones, B. Safdi, and J. Ye, "Broadband cavity ringdown spectroscopy for sensitive and rapid molecular detection," Science **311**(5767), 1595–1599 (2006).
4. W. C. Swann and N. R. Newbury, "Frequency-resolved coherent lidar using a femtosecond fiber laser," Opt. Lett. **31**(6), 826–828 (2006).
5. T. Udem, J. Reichert, R. Holzwarth, and T. W. Hänsch, "Absolute optical frequency measurement of the Cesium D_1 line with a mode-locked laser," Phys. Rev. Lett. **82**(18), 3568–3571 (1999).
6. A. A. Madej, L. Marmet, and J. E. Bernard, "Rb atomic absorption line reference for single Sr^+ laser cooling systems," Appl. Phys. B **67**(2), 229–234 (1998).
7. H. S. Moon, E. B. Kim, S. E. Park, and C. Y. Park, "Selection and amplification of modes of an optical frequency comb using a femtosecond laser injection-locking technique," Appl. Phys. Lett. **89**(18), 181110 (2006).
8. L.-S. Ma, Z. Bi, A. Bartels, L. Robertsson, M. Zucco, R. S. Windeler, G. Wilpers, C. Oates, L. Hollberg, and S. A. Diddams, "Optical frequency synthesis and comparison with uncertainty at the $10^{(-19)}$) level," Science **303**(5665), 1843–1845 (2004).
9. Y.-J. Kim, J. Jin, Y. Kim, S. Hyun, and S.-W. Kim, "A wide-range optical frequency generator based on the frequency comb of a femtosecond laser," Opt. Express **16**(1), 258–264 (2008).

#278682 http://dx.doi.org/10.1364/OE.25.000681
Journal © 2017 Received 12 Oct 2016; accepted 23 Dec 2016; published 10 Jan 2017

Optics EXPRESS

10. H. Y. Ryu, S. H. Lee, W. K. Lee, H. S. Moon, and H. S. Suh, "Absolute frequency measurement of an acetylene stabilized laser using a selected single mode from a femtosecond fiber laser comb," Opt. Express **16**(5), 2867–2873 (2008).
11. http://www.menlosystems.com/assets/documents-2/FC1500-ProductBrochure.pdf
12. K. J. Vahala, "Optical microcavities," Nature **424**(6950), 839–846 (2003).
13. P. Del'Haye, A. Schliesser, O. Arcizet, T. Wilken, R. Holzwarth, and T. J. Kippenberg, "Optical frequency comb generation from a monolithic microresonator," Nature **450**(7173), 1214–1217 (2007).
14. T. J. Kippenberg, R. Holzwarth, and S. A. Diddams, "Microresonator-based optical frequency combs," Science **332**(6029), 555–559 (2011).
15. K. Saha, Y. Okawachi, B. Shim, J. S. Levy, R. Salem, A. R. Johnson, M. A. Foster, M. R. E. Lamont, M. Lipson, and A. L. Gaeta, "Mode locking and femtosecond pulse generation in chip-based frequency combs," Opt. Express **21**(1), 1335–1343 (2013).
16. V. B. Braginsky, M. L. Gorodetsky, and V. S. Ilchenko, "Quality-factor and nonlinear properties of optical whispering-gallery modes," Phys. Lett. A **137**(7–8), 393–397 (1989).
17. A. A. Savchenkov, A. B. Matsko, V. S. Ilchenko, and L. Maleki, "Optical resonators with ten million finesse," Opt. Express **15**(11), 6768–6773 (2007).
18. W. Liang, D. Eliyahu, V. S. Ilchenko, A. A. Savchenkov, A. B. Matsko, D. Seidel, and L. Maleki, "High spectral purity Kerr frequency comb radio frequency photonic oscillator," Nat. Commun. **6**, 7957 (2015).
19. V. S. Ilchenko, A. A. Savchenkov, A. B. Matsko, and L. Maleki, "Generation of Kerr frequency combs in a sapphire whispering gallery mode microresonator," Opt. Eng. **53**(12), 122607 (2014).
20. I. M. White, J. D. Suter, H. Oveys, X. Fan, T. L. Smith, J. Zhang, B. J. Koch, and M. A. Haase, "Universal coupling between metal-clad waveguides and optical ring resonators," Opt. Express **15**(2), 646–651 (2007).
21. X. Zhang and A. M. Armani, "Silica microtoroid resonator sensor with monolithically integrated waveguides," Opt. Express **21**(20), 23592–23603 (2013).
22. T. J. Kippenberg, S. M. Spillane, and K. J. Vahala, "Kerr-nonlinearity optical parametric oscillation in an ultrahigh-Q toroid microcavity," Phys. Rev. Lett. **93**(8), 083904 (2004).
23. T. Herr, V. Brasch, J. D. Jost, I. Mirgorodskiy, G. Lihachev, M. L. Gorodetsky, and T. J. Kippenberg, "Mode spectrum and temporal soliton formation in optical microresonators," Phys. Rev. Lett. **113**(12), 123901 (2014).
24. M. Erkintalo and S. Coen, "Coherence properties of Kerr frequency combs," Opt. Lett. **39**(2), 283–286 (2014).
25. W. Liang, V. S. Ilchenko, D. Eliyahu, A. A. Savchenkov, A. B. Matsko, D. Seidel, and L. Maleki, "Ultralow noise miniature external cavity semiconductor laser," Nat. Commun. **6**, 7371 (2015).
26. A. B. Matsko and L. Maleki, "On timing jitter of mode-locked Kerr frequency combs," Opt. Express **21**(23), 28862–28876 (2013).
27. A. A. Savchenkov, D. Eliyahu, W. Liang, V. S. Ilchenko, J. Byrd, A. B. Matsko, D. Seidel, and L. Maleki, "Stabilization of a Kerr frequency comb oscillator," Opt. Lett. **38**(15), 2636–2639 (2013).
28. A. C. Bordonalli, C. Walton, and A. J. Seeds, "High-performance homodyne optical injection phase-lock loop using wide-linewidth semiconductor lasers," IEEE Photonics Technol. Lett. **8**(9), 1217–1219 (1996).
29. K. Balakier, M. J. Fice, L. Ponnampalam, A. J. Seeds, and C. C. Renaud, "Monolithically integrated optical phase-lock loop for microwave photonics," J. Lightwave Technol. **32**(20), 3893–3900 (2014).
30. C. C. Renaud, M. Duser, C. F. C. Silva, B. Puttnam, T. Lovell, P. Bayvel, and A. J. Seeds, "Nanosecond channel-switching exact optical frequency synthesizer using an optical injection phase-locked loop (OIPLL)," IEEE Photonics Technol. Lett. **16**(3), 903–905 (2004).
31. C. C. Renaud, C. F. C. Silva, M. Dueser, P. Bayvel, and A. J. Seeds, "Exact, agile, optical frequency synthesis using an optical comb generator and optical injection phase-lock loop," in *Digest of the LEOS Summer Topical Meetings* (2003), paper WC1.3/67.
32. H. Inaba, T. Ikegami, H. Feng-Lei, A. Onae, Y. Koga, T. R. Schibli, K. Minoshima, H. Matsumoto, S. Yamadori, O. Tohyama, and S. I. Yamaguchi, "Phase locking of a continuous-wave optical parametric oscillator to an optical frequency comb for optical frequency synthesis," IEEE J. Quantum Electron. **40**(7), 929–936 (2004).
33. T. R. Schibli, K. Minoshima, E. L. Hong, H. Inaba, Y. Bitou, A. Onae, and H. Matsumoto, "Phase-locked widely tunable optical single-frequency generator based on a femtosecond comb," Opt. Lett. **30**(17), 2323–2325 (2005).
34. J. E. Bowers, A. Beling, A. Bluestone, S. M. Bowers, L. Chang, S. Diddams, G. Fish, T. Kippenberg, T. Komljenovic, E. Norberg, S. Papp, K. Srinivasan, L. Theogarajan, K. Vahala, and N. Volet, "Chip-scale optical resonator enabled synthesizer (CORES): Miniature systems for optical frequency synthesis," in *IEEE International Frequency Control Symposium (IFCS)* (2016), pp. 1–5.
35. L. Mingzhi, P. Hyun-chul, E. Bloch, A. Sivananthan, J. S. Parker, Z. Griffith, L. A. Johansson, M. J. W. Rodwell, and L. A. Coldren, "An integrated 40 gbit/s optical costas receiver," J. Lightwave Technol. **31**(13), 2244–2253 (2013).
36. S. Ristic, A. Bhardwaj, M. J. Rodwell, L. A. Coldren, and L. A. Johansson, "An optical phase-locked loop photonic integrated circuit," J. Lightwave Technol. **28**(4), 526–538 (2010).
37. M. Lu, H.-C. Park, E. Bloch, L. A. Johansson, M. J. Rodwell, and L. A. Coldren, "A highly-integrated optical frequency synthesizer based on phase-locked loops," *Optical Fiber Communication Conference 2014* (2014).
38. J. Parker, M. Lu, H. Park, E. Bloch, A. Sivananthan, Z. Griffith, L. A. Johansson, M. J. Rodwell, and L. A. Coldren, "Offset locking of an SG-DBR to an InGaAsP/InP mode-locked laser," in *IEEE Photonics Conference (IPC)* (2012).

Optics EXPRESS

39. J. Parker, A. Sivananthan, M. Lu, L. Johansson, and L. Coldren, "Integrated phase-locked multi-THz comb for broadband offset locking," in OSA Technical Digest, *Optical Fiber Communication Conference* (2012), paper OM3E.5.
40. M. Lu, "Integrated optical phase-locked loops," in *Electrical and Computer Engineering*, University of California, Santa Barbara (2013) p. 252.
41. http://www.adsantec.com/200-asnt5020-pqc.html http://www.adsantec.com/83-asnt5040-kmc.html
42. R. J. Steed, F. Pozzi, M. J. Fice, C. C. Renaud, D. C. Rogers, I. F. Lealman, D. G. Moodie, P. J. Cannard, C. Lynch, L. Johnston, M. J. Robertson, R. Cronin, L. Pavlovic, L. Naglic, M. Vidmar, and A. J. Seeds, "Monolithically integrated heterodyne optical phase-lock loop with RF XOR phase detector," Opt. Express **19**(21), 20048–20053 (2011).

1. Introduction

There has been recent and extensive research in the development of optical frequency synthesizers (OFSs) with applications including absolute optical frequency measurements [1], optical spectroscopy [2], gas sensing [3], light detection and ranging (LiDAR) [4], and optical frequency metrology [5, 6]. Despite their widespread potential applications, at present optical frequency synthesizers have found only limited use due to their cost, size, weight, and dc power requirements.

Considering this, realization of a compact, inexpensive, and low-power OFS is a key requirement. These goals suggest highly-integrated chip scale designs. However, it is challenging to integrate various optical and electronic devices on the same chip. Low power consumption is especially important because thermal cross-talk and associated thermal management may prevent the tight integration of the optical components.

An OFS includes several key elements. An optical frequency comb must be locked to an optical clock. This comb defines the frequency of the generated optical signal. Also required is a broadly tunable laser or bank of lasers that are referenced to the optical frequency comb. Finally, efficient and agile electronic circuits are needed to offset lock the laser to the frequency comb.

Despite being fully-locked and referenced, commercially-available optical frequency synthesizers involve bulk optics and electronics consuming power on the order of kW. This power is primarily consumed by the optical frequency comb generators. Mode-locked femtosecond optical frequency combs lay in the core of the OFS approaches [7–10]. Commercially available systems based on titanium sapphire or fiber laser based femtosecond mode-locked lasers are 0.14 m^3 in volume and consume 0.5 kW power [11].

The problem of the power-efficient optical frequency comb generator can be solved using optical microresonators [12]. Microresonator-based Kerr frequency combs belong to the class of frequency comb generators that lend themselves for on-chip integration [13]. An added advantage is that compared to traditional mode-locked or femtosecond laser-based optical frequency comb (OFC), a microresonator-based comb uses few hundreds of mW power, and provides ultralow noise and phase-coherent output with spectral linewidths on the order of sub-Hz. While monolithic planar resonators integrated on various platforms and producing the frequency combs were demonstrated [14, 15], none of them were integrated with the pump laser, and hence none of them represent complete chip-scale devices. The reason is that the power required to produce the frequency combs is usually in hundreds of mW range, which makes the chip integration impractical. The large power consumption by the laser as well as significant attenuation of the pump light in the microresonator complicates the thermal management of the system as the whole. To reduce the power consumption, one needs high quality (*Q*-) factor microresonators.

The frequency comb generator is based on the crystalline whispering gallery mode (WGM) resonator that has the following salient advantages over other devices of this kind [16, 17]. Firstly, it has low intrinsic loss (if overloaded) and high intrinsic *Q*-factor [17]. As the result, it is possible to reduce absorption of the light in the resonator. Secondly, the resonator has outstanding thermo-mechanical properties that allow realizing ultranarrow linewidth lasers on a chip using self-injection locking of the laser to the resonator. The optical

Optics EXPRESS

frequency comb oscillator benefits from the laser and, as the result, the relative optical stability of each comb harmonic does not exceed 10^{-10} at 1 sec [18]. Thirdly, high optical *Q* allows reducing fundamental noises of the Kerr comb oscillator. The noises are further reduced since proper design of the resonator morphology results in increase of the volume of the optical mode need for reduction of the thermodynamic noise associated with the resonator. Fourthly, the resonator has small mass and large mechanical Q that reduces its acceleration and vibration sensitivity [19]. This feature is supported by the low acceleration sensitivity of the whole oscillator platform. Despite the fact that WGM resonators were created on a chip, the efficient planar couplers are yet to be developed for them. Preliminary studies show that it is possible [20, 21].

The Kerr frequency comb generated in the microresonator results from the process of four-wave mixing [22]. The comb emerges when the pump power, produced by the continuous-wave laser self-injection locked to a mode of the resonator, exceeds a certain threshold. The resonator is characterized with the ultimate anomalous group velocity dispersion and supports formation of the intracavity dissipative solitons [23]. The frequency comb stability is defined by the stability of the pump light, on one hand, and the repetition rate of the soliton train, on the other. Both values are extremely good. As the result, the whole oscillator represents an ultimate reference for creation of the OFS.

The OFC coherence can change through its spectrum, resulting a broader spectral linewidth for comb components that are away from the pump wavelength [24]. However, for a practically realizable spectrally narrow mode-locked Kerr frequency comb, this is not the case as the phase noise of the comb repetition rate is low [18], if compared with the properly normalized noise of the pump laser [25]. Moreover, in an ideal case, the repetition-rate noise of the Kerr frequency comb does not depend on the pump laser noise and can be extremely low [26, 27]. It means that for the narrow OFC reported here, we can neglect repetition rate induced phase noise and assume that all the optical harmonics have sub-Hz linewidth corresponding to the pump laser.

An optical frequency comb generates a series of discrete optical frequency harmonics, whereas an OFS has to provide a continuous tuning of the optical frequency. To realize this functionality, one needs a widely tunable laser that can be frequency locked to the optical frequency comb. There are several locking approaches such as optical injection locking (OIL), optical injection phase-lock loop (OIPLL) and optical phase-lock loop (OPLL) to achieve this functionality. Optical frequency synthesis with a wide tuning range is not possible using OIL approach alone due to the system instability above critical injection levels [28, 29]. Moreover, OIL is purely a homodyne technique, which does not allow for continuous tuning of an offset between the slave laser and the comb. Continuous tuning over a wide range of frequencies was achieved through the combination of OIL and OPLL technologies [30, 31]. However, such a hybrid system increases the system complicacy and the issue of offset tunability still remains.

Phase locking a tunable local oscillator to the OFC using chip scale OPLLs is, therefore, considered as the most popular ways of achieving OFSs [32–34]. With the developments in PIC and electronic IC integration, small loop delays and large loop bandwidths; realization of OPLLs is a more appealing solution compared to OIL, and OIPLL [35]. OFSs with accurate and stable optical output phase-locked to a phase-coherent and ultra-low linewidth optical reference with feedback control in the radio frequency (RF) domain can be utilized in the devices. The so-called heterodyne OPLL [36] is the concept by which chip scale and highly integrated OFSs were demonstrated, where the OFC with spectral span ~3 nm was generated with a modest linewidth of 100 kHz external-cavity laser and two cascaded modulators [37]. In addition, similar type of frequency synthesis was shown by offset locking a widely tunable on-chip laser to mode-locked laser comb, which also needs to be stabilized by second phase locking to a narrow-linewidth reference laser [38, 39], introducing more complexity. All of

Optics EXPRESS

these solutions are power hungry, difficult to integrate and complex unlike the work reported here.

In this paper, we report on the experimental demonstration of a chip scale optical frequency synthesizer achieved by offset-locking an on-chip widely tunable sampled-grating distributed-Bragg-reflector (SG-DBR) laser to a magnesium fluoride (MgF_2) microresonator-based optical frequency comb with a 50-dB span of 25 nm (~3 THz) around 1550 nm and ~26 GHz repetition rate. The reference frequency comb generator used in the chip-scale OFS represent an example of fully heterogeneously integrated Kerr frequency comb generator. The physical package of the device, that includes the pump laser, the optical coupling element, the high-*Q* microresonator, and support electronics and thermal control has volume less than 0.2 cm^3 and total electric power consumption of 400 mW. This study also reports the demonstration of tuning between comb lines with a tunable RF synthesizer for offset locking. Tuning resolution better than 100 Hz within ± 5 Hz accuracy is also accomplished. As a further evaluation of our OFS, the frequency switching time with a wavelength separation >5 nm by jumping over 28 comb lines is also experimentally measured. The total power consumption of the entire OFS system is roughly 2 W (excluding EDFA). To the best of our knowledge, this is the first demonstration of a chip scale OFS with fastest switching time between the comb lines, highest tuning resolution and lowest power consumption.

This paper is organized as follows. This paper begins with a discussion on the concept of the OFS, design of highly integrated heterodyne OPLL and operation of Kerr frequency comb generation. We then describe the experimental setup used for offset locking to OFC and the corresponding results. Finally, the measured metrics of the chip-scale OFS are introduced.

2. Concept and design of frequency synthesis

The basic idea of a compact and chip-scale OFS is illustrated in Fig. 1. A microresonator-based OFC is used as the ultra stable and narrow linewidth source, serving as a master laser. The comb lines are then used as the reference for the heterodyne OPLL. A RF frequency f_{RF} from a tunable RF synthesizer is applied to feedback electronic circuits of the OPLL to introduce a frequency offset. By tuning the phase section current of the slave laser as well as f_{RF}, the slave laser is phase-locked to the comb lines. The two basic requirements to be met in order for an OFS to cover all the frequencies between comb lines are: (i) the heterodyne OPLL offset frequency range must be at least half of the comb's free-spectral-range (FSR), and (ii) the FSR of the comb must be less than the slave laser's mode-hop free tuning range. In such a way, continuous tuning is achieved.

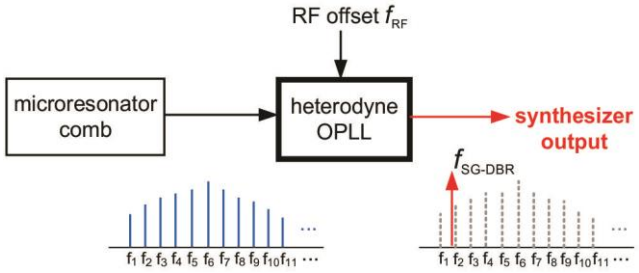

Fig. 1. Optical frequency synthesizer system, showing two main building blocks – a comb source and a heterodyne OPLL. The optical spectra are also plotted at the output of each block.

From the two building blocks of the OFS shown in Fig. 1, a more detailed view of the thick-lined rectangle block, labelled as heterodyne OPLL, is displayed in Fig. 2. The heterodyne OPLL system consists of a photonic integrated circuit (PIC) and feedback electronic circuits. The latter is composed of electronic ICs (EICs) and a loop filter. The master (injected single comb line in this case) and slave lasers in a PIC oscillate at different frequencies, producing a beat signal at this offset frequency on the balanced photodetector

Optics EXPRESS

pair. The beat signal is then amplified by the limiting amplifier (LIA) to make the system insensitive to intensity fluctuation from the PIC. In other words, LIA limits the optical beat note signal to logic values so that system is unresponsive to any changes in optical intensity. A phase detector (logic XOR gate in this case) compares the phase of the beat signal with a reference signal from a tunable RF synthesizer, thus generating the baseband phase error signal. This is then fed back through the loop filter to control the slave laser phase and hence lock the phase of the slave laser to a single comb line.

Figure 3 shows an optical microscope photo of the heterodyne OPLL system board where PIC, EIC and LF were assembled closely together by wirebonding. The inset shows the picture of the test bench. The PIC consists of a widely tunable sampled-grating distributed Bragg reflector (SG-DBR) laser, a 2 × 2 multi-mode interference (MMI) coupler, a couple of semiconductor optical amplifiers (SOAs) to preamplify the input comb lines, two high-speed quantum well (QW)-based waveguide photodetectors (PDs), all integrated on an InGaAsP/InP platform. The on-chip SG-DBR laser has a wavelength tuning range of 40 nm.

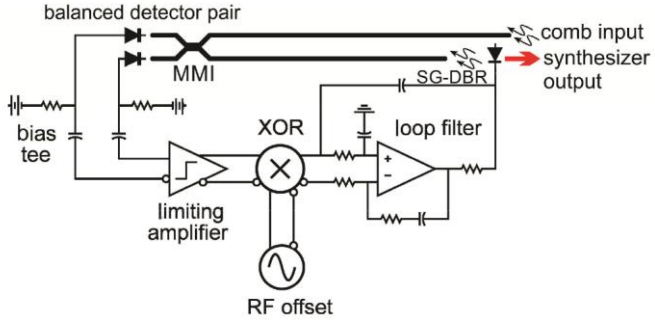

Fig. 2. System architecture of the heterodyne OPLL-based widely tunable OFS.

With a −3 V bias, the 3-dB RF bandwidth of the QW PDs can be as high as 14 GHz [40]. For the high-speed LIA and logic XOR gate, commercial-off-the-shelf (COTS) SiGe elements were employed for the electronics part, whereas discrete surface-mount device (SMD) components were used to build up the loop filter circuit whose loop bandwidth is designed to be ~400 MHz. LIA has a differential gain about 30 dB with a 3-dB bandwidth of 17 GHz. XOR can work at least up to 13 GHz input clock frequencies. The details of these COTS ICs can be found in [41]. The OPLL system size is around 1.8 × 1.6 cm^2. A 24-pin dc probe card was used to power up the OPLL system, and two 2signal-line GSGSG RF probes were used to monitor the device performance and supply the RF offset reference signal to the XOR. The maximum offset frequency our OPLL can lock the tunable laser to a reference laser at was verified to be as high as 15.6 GHz, clearly allowing the OFS to be continuously tuned.

3. Kerr frequency comb generation

To create the Kerr frequency comb generator, we fabricated a high-*Q* MgF2 whispering gallery mode resonator (WGMR) out of a cylindrical crystalline preform using mechanical grinding and polishing. The resonator is approximately 2.7 mm in diameter and 0.1 mm in thickness. The intrinsic optical *Q*-factor of the resonator exceeded 5 × 10^9. The resonator was characterized with a FSR of 25.7 GHz and anomalous group velocity dispersion resulting in 3 kHz difference between two adjacent FSRs.

The resonator was integrated with two coupling prisms and the loaded *Q*-factor was reduced to 5 × 10^8. The over coupling of the WGMR is useful for reduction of the thermal instabilities of the resonator occurring because of the light attenuation in the resonator host material.

Optics EXPRESS

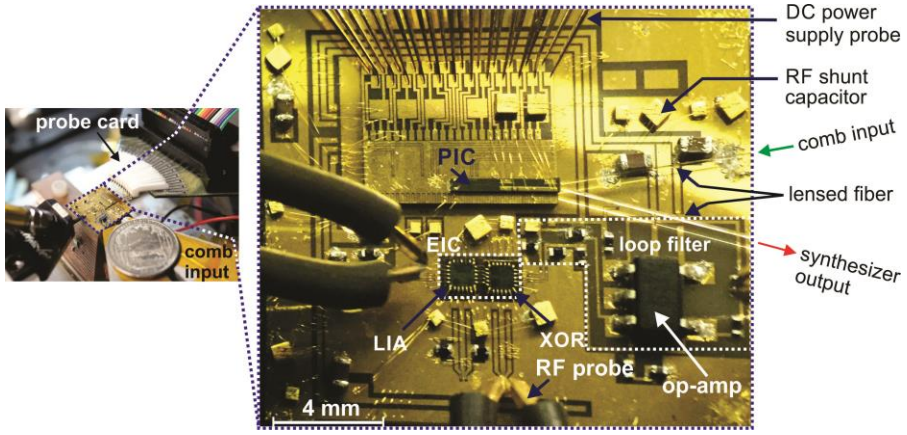

Fig. 3. The heterodyne OPLL on the test bench where the US quarter shown as a scale (right). A close-up view of the heterodyne OPLL board (left). The PIC, EIC and loop filter are labeled.

Light emitted by a semiconductor distributed feedback (DFB) laser was collimated and send to the resonator. When the light hit a WGM, the laser frequency was locked to the mode due to the optical feedback from the mode occurring because of resonant Rayleigh scattering. As the result of the locking the linewidth of the laser reduced to a sub-kHz level. As illustrated in Fig. 4(a), the light exiting the resonator through add and drop prism couplers was sent to a fast RF photodiode and an output optical coupler, respectively.

When the laser power exceeded a certain threshold (approximately 3 mW laser power corresponding to 1 mW in the mode) the unit produced a coherent frequency comb operating in the self-injection locked regime. The demodulating the frequency combs on a fast photodiode results in spectrally pure RF signal. Figure 4(d) shows the measured optical spectrum of the generated comb in the C-band under 20 mW laser power. The total power output from the fiber is ~335 μW and the comb envelope is 15 dB lower than the carrier.

Optics EXPRESS

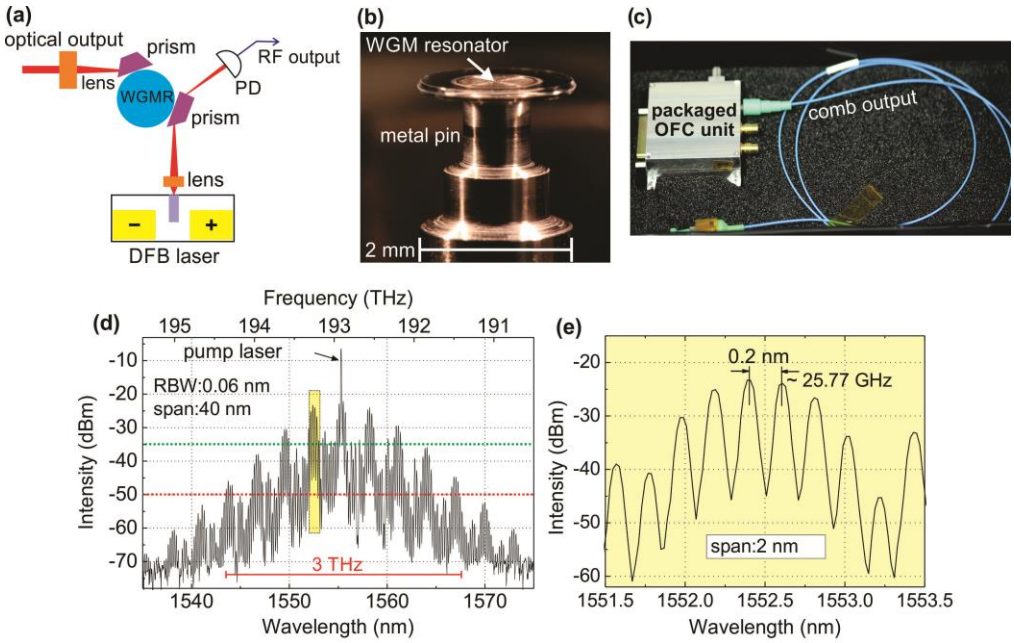

Fig. 4. (a) Schematic diagram of the set-up of the optical frequency comb (OFC) in a MgF_2 crystalline whispering gallery mode (WGM) resonator. The distributed feedback (DFB) laser pumps the resonator using an evanescent wave prism coupler. The generated frequency comb leaves the resonator through prism couplers. The light exiting one of the prism couplers was sent to a fast RF photodiode and optical output was obtained from the other coupler, (b) optical microscope image of the MgF_2 crystal forming optical WGM resonators, (c) packaged OFC unit with green fiber pigtail, (d) optical spectrum of a stabilized Kerr frequency combs (left) generated in the unit (right). The comb spans 3 THz defined as the width where the intensity ≥ 50 dBm (red dotted line) and has a line spacing of 25.7 GHz, yielding more than 115 lines. The optical output comb power exiting the fiber (greenjacketed) is 100 μW obtained after subtracting from the pump laser power, meaning only ~0.5 μW per comb line is achieved in the wavelength range of 1535 nm-1575 nm. The horizontal (green) dashed line denotes the 0.5 μW per comb line power level. (e) Clearly observed lines of a multi-soliton Kerr frequency comb with a spacing of 0.2 nm.

4. Experimental setup

The comb output from the packaged and fiber-pigtailed OFC unit goes through an erbium-doped fiber amplifier (EDFA) and finally coupled into the OPLL PIC using lensed fiber. The power requirement per comb line for stable offset-locking is measured to be 20 μW (17 dBm) in the fiber near 1550 nm operating wavelength. As the comb output is only 10 dBm in the fiber and divided over several comb lines, the EDFA is necessary to provide adequate power levels. The SG-DBR laser signal was coupled out from the back mirror and through a short semiconductor optical amplifier (SOA) using similar lensed fiber for monitoring purposes. To measure the OPLL tone, the output from the SGDBR was mixed with the comb in a 2 × 2 coupler, detected via an external high speed photodetector, and measured on an electrical signal analyzer (ESA), as shown in Fig. 5. The other output of this coupler is connected to the optical spectrum analyzer (OSA) to measure the optical spectra of SG-DBR laser and the comb output. Note that the linewidth of the unlocked SG-DBR is on the order of 10 MHz. A signal with a frequency equal to the beat note frequency, f_{RF} as frequency offset is applied from the RF synthesizer to XOR within the EIC.

Optics EXPRESS

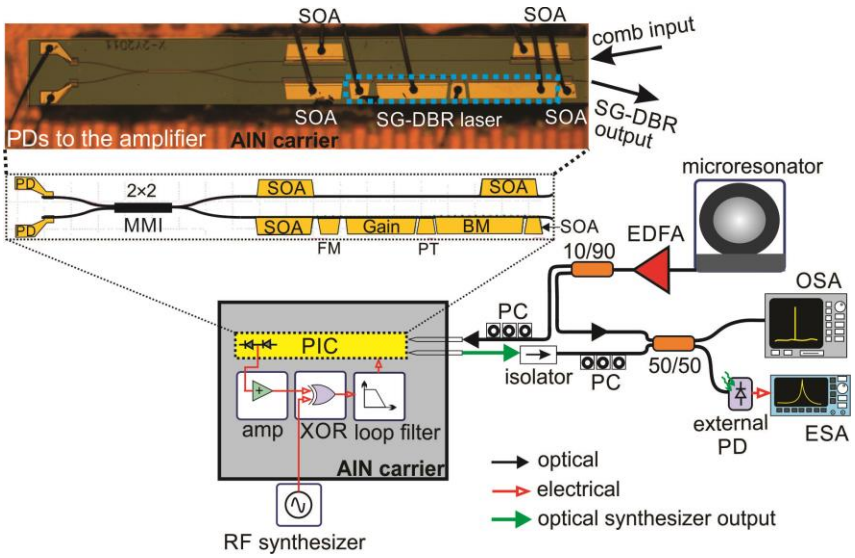

Fig. 5. The test setup of the optical synthesizer using heterodyne OPLL locking scheme. A microscope picture of the fully fabricated PIC mounted on AlN carrier with wirebonding shown at the top. (amp: amplifier, BM: back mirror, ESA: electrical spectrum analyzer, EDFA: erbium doped fiber amplifier, FM: front mirror, MMI: multimode interference, OSA: optical spectrum analyzer, PC: polarization controller, PT: phase tuner, PD: photodetector, PIC: photonic integrated circuit, SOA: semiconductor optical amplifier).

5. Results and discussion

5.1 Offset locking to comb lines

The phase-locking of the SG-DBR laser to the comb lines is achieved. Figure 6 shows the optical and electrical spectra when two lasers are phase-locked with an offset frequency of 11 GHz. The combined optical spectra of the SG-DBR and the comb lines are shown in Fig. 6(a) where both light source peaks around 1562 nm with a wavelength separation of 0.09 nm are seen. Since the OFC lines are uneven in amplitude, and they are roughly equally amplified by EDFA, some of the lines are buried by the amplified spontaneous emission (ASE) noise floor. The RF spectra of the beat note at an offset frequency of 11 GHz, in cases of locked and free running, are shown in Fig. 6(b). In the locked case, the RF linewidth is reduced significantly, indicating the coherence between the SG-DBR laser and comb. The beat tone generated between the locked SG-DBR and the adjacent comb line is seen at 14.7 GHz (i.e. 25.7 ± 11 GHz). This is expected, since comb lines are stable in phase with respect to each other and the OPLL is phase-locked to the central comb line, hence the OPLL is phase-locked to the adjacent comb line. Also, the RF beat tone produced between comb lines is observed at 25.7 GHz (not shown).

Optics EXPRESS

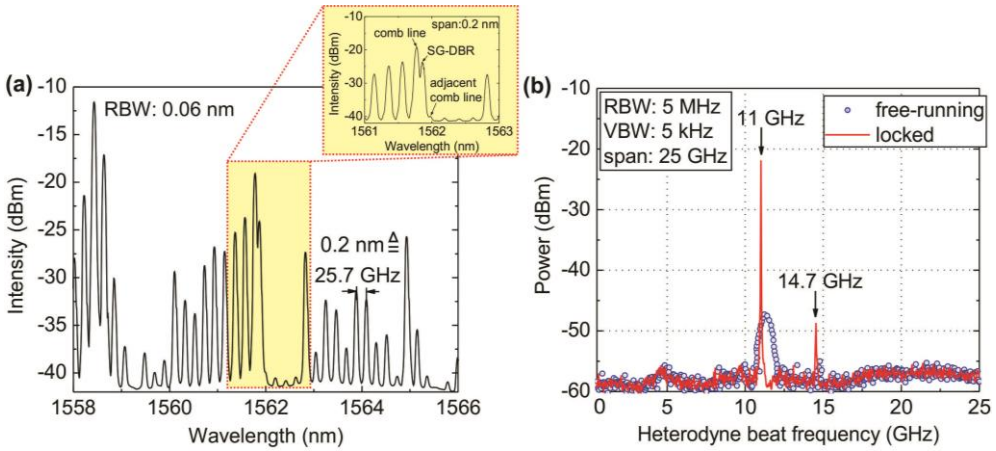

Fig. 6. (a) Optical spectrum when SG-DBR laser and comb are phase locked with a frequency difference of 11 GHz. The locking is to the comb line at 1561.77 nm. The zoom-in spectrum with a span of 2 nm is shown as inset, and (b) the RF spectrum, showing the locked beat note between SG-DBR and comb at 11 GHz is recorded. The beat note generated between SG-DBR and adjacent comb line is also visible. Both the phase-locked and free-running cases are shown to illustrate the improved relative spectral coherence between the on-chip tunable laser and comb.

5.2 Tuning resolution of OFS

The RF signal generated by beating between comb lines on a fast PD was measured. An exceptionally high spectrally pure RF line, as shown in Fig. 7(b), is observed. The 3-dB beat width of the RF tone at 25.7 GHz is <100 Hz, limited by the resolution bandwidth (RBW) of the ESA. This clearly suggests that this ultra-narrow linewidth and frequency stabilized OFC itself could be used as a reference light source for measuring the tuning resolution of our developed OFS. As a part of the experiment, the OFS output from our integrated OPLL system was mixed with the phase-coherent OFC output. As can be seen in Fig. 7(a), the mixed optical outputs are then beat down to a RF frequency by detecting that light on a high-speed external PD for precise measurement. The RF synthesizer connected to the XOR of our OPLL system was tuned in by a number of 100 Hz steps. The RF spectra were then recorded using ESA when the optical beat note is offset-locked at 2.5 GHz, as displayed in Fig. 7(c). The output optical beat note frequency shift $\Delta f_{\text{optical}}$ was then plotted as a function of change in RF frequency Δf_{RF} (Fig. 7(d)). Deviation from 100 Hz is observed to be on the order of ± 5 Hz. In such a way, our optical synthesizer achieves sub-100 Hz tuning resolution, which is the highest resolution so far reported for a chip-scale OFS. It should be noted that the optical beat note, shown in Fig. 7(c), is formed by beating the locked laser to the reference laser, indicating relative linewidth between these two light sources.

Optics EXPRESS

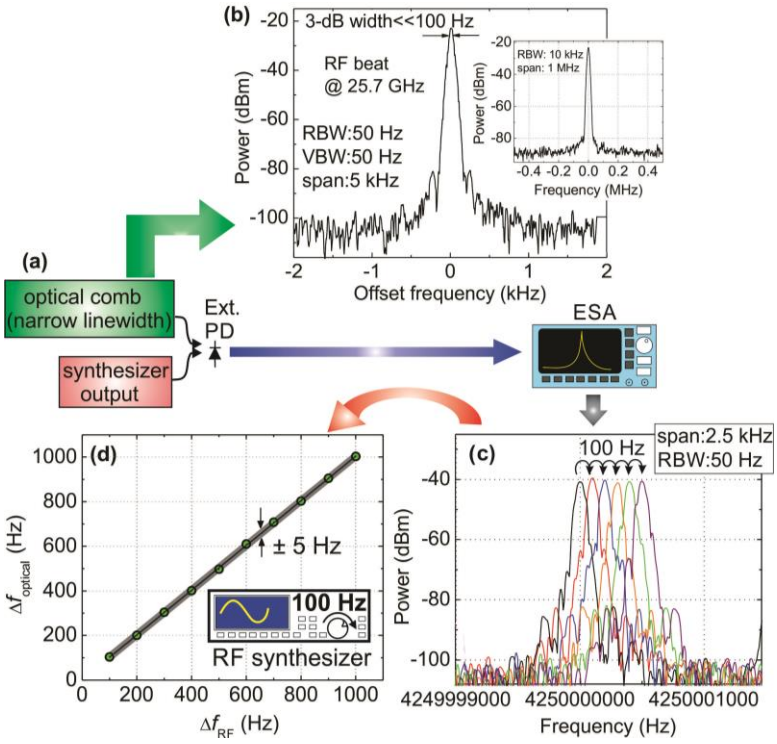

Fig. 7. (a) The measurement setup for the tuning resolution of our OFS, (b) Power spectra of an RF frequency signal at 25.7 GHz generated by beating between comb lines on a high-speed PD integrated in the packaged unit measured with different resolution bandwidth. The smaller peaks are of 60 Hz and its harmonics, appearing from the power source, (c) locked beat signal between reference comb line and the SG-DBR laser and its movement by 100 Hz, and (d) plot of change in the optical beat note with respect to change in the RF offset frequency.

5.3 Switching speed of OFS

Figure 8(a) shows how switching speed measurements of our OFS were performed. The front mirror section of the SG-DBR laser was modulated by square wave signal with a frequency of 800 kHz and 50% duty cycle from a function generator; whereas the back mirror remained open. A bias tee was used to add such a time-varying signal upon the dc bias. The square-wave signal into the front mirror modulates the lasing wavelength between two values with a separation of 5.6 nm. The peak-to-peak amplitude of modulation current applied into the front mirror was 1.6 mA measured using current probe. Laser output was then passed onto manually tunable bandpass optical filter with a 3dB bandwidth 0.95 nm, which allows only one wavelength component to pass through. Optical signals were then detected by an external high-speed photodetector and the traces on the real-time oscilloscope were analyzed. When the modulation is on, the wavelength is switched between two values separated by 5.6 nm at 800 kHz speed, which is much faster than spectrum capturing rate the optical spectrum analyzer (OSA). Therefore, both wavelength values on the OSA are observed simultaneously, as shown in Fig. 8(b). The dc offset and amplitude of the square wave are carefully selected in a way so that two output wavelengths of SG-DBR lasers can beat against two comb lines with a reasonably good optical intensity and generate a RF beat note with the same frequency. The superimposed optical spectra of comb output and laser at these two specific states are shown in Fig. 8(c). Note that the oscilloscope was triggered with the sync. output signal of the function generator. The wavelength separation between the two peaks of SG-DBR laser and comb output in two different spectral regions is 0.024 nm, corresponding to an offset frequency ~2.5 GHz, when they beat with each other.

Optics EXPRESS

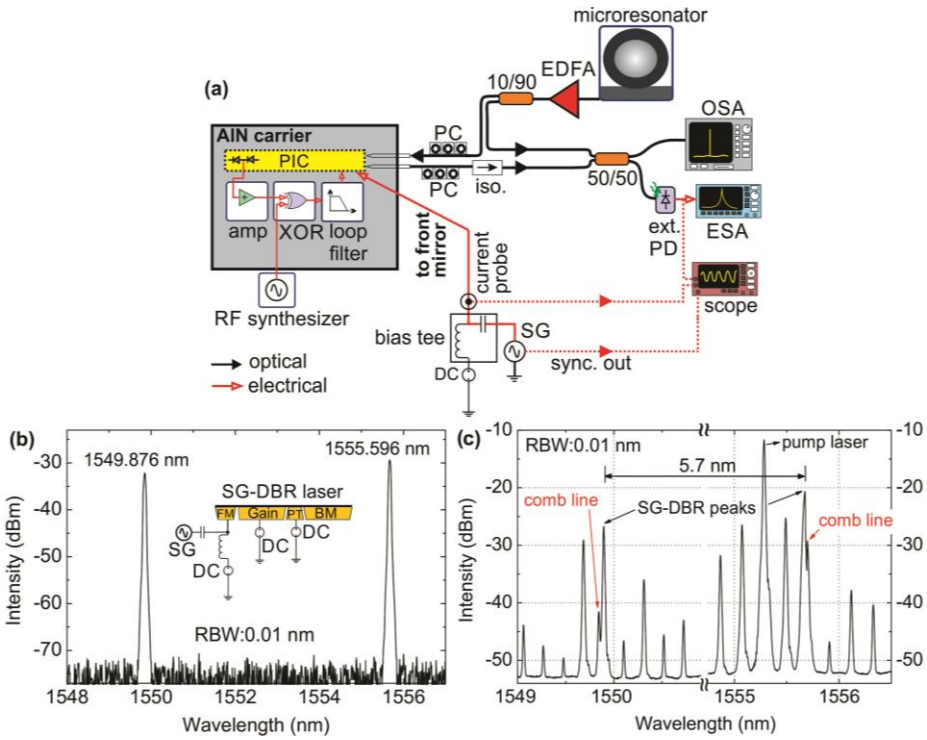

Fig. 8. (a) The test setup for measuring the switching speed of our OFS, (b) the optical spectrum of SG-DBR laser when the front mirror is modulated by a 800 kHz square-wave from a signal generator and gain current is set to a constant value of 130 mA, resulting wavelength switching between $\lambda_{1,SG\text{-}DBR}$ = 1549.876 nm and $\lambda_{2,SGDBR}$ = 1555.596 nm, and (c) superimposed optical spectra of comb output and SG-DBR laser, where both comb peaks separated by 0.024 nm from their corresponding SG-DBR laser peaks can be resolved. (BM = back mirror, DC = direct current, EDFA = erbium doped fiber amplifier, ext. PD = external photodetector, FM = front mirror, PIC = photonic integrated circuit, PC = polarization controller, PT = phase tuner, RBW = resolution bandwidth)

During the wavelength switching of SG-DBR laser, the electrical spectrum measured in ESA is shown in Fig. 9. The sharp single peak at an offset frequency of 2.5 GHz generated between SG-DBR and comb lines around 1550 nm and 1555 nm is the clear evidence for phase locking of on-chip noise lasers to comb output. The beating tone between the SG-DBR laser and the adjacent comb lines at 23.2 GHz as well as the tone at 25.7 GHz between comb lines are also seen here.

Optics EXPRESS

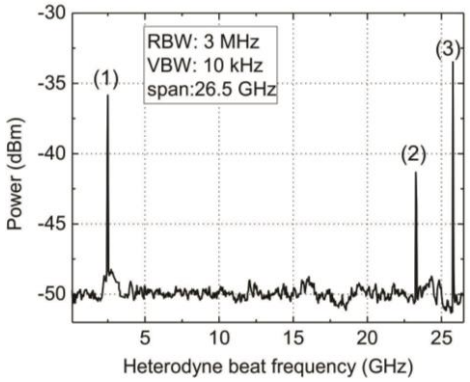

Fig. 9. RF spectrum measured at the ESA of modulated SG-DBR laser beating with the comb output during dynamic wavelength switching of SG-DBR. Three peaks are seen, (1) the locked beat note is at 2.5 GHz, produced by beating between both SGDBR peaks and the corresponding comb lines, (2) The beat note generated between both SG-DBR peak and adjacent corresponding comb line is at 23.3 GHz, and (3) the beat note produced between comb lines is at 25.7 GHz.

The OPLL will lock the on-chip SG-DBR laser to comb when the whole system including the right offset frequency from the RF synthesizer is on. This is clearly evidenced by Fig. 8(c) and 9 where one can see that two wavelengths of SG-DBR line up with two lines of the comb, generating single sharp RF beat note at 2.5 GHz. This time the output of the external PD is monitored on a wide-bandwidth real-time oscilloscope instead of connecting with ESA, illustrated by the dotted electrical path shown in Fig. 8(a). The oscilloscope trace, displayed in Fig. 10, is showing that the SG-DBR laser is phase-locked most of the time except for a short period of OPLL transient time. Importantly, this is happening periodically at a modulation frequency 800 kHz. The time interval in between two high states of such a trace can be considered as wavelength switching of SG-DBR and OPLL locking time, which is extracted as 200 ns. In the time interval of phase locking, a sinusoidal signal at 2.5 GHz, representing the locked beat note, is observed, which is shown in Fig. 10(b). Hence, our synthesizer achieves sub-μs switching and locking time.

5.4 Phase noise measurement

To evaluate the performance of our OPLL system using COTS ICs, residual phase noise of the OPLL was measured from 10 Hz to 1 GHz using the setup shown in Fig. 5. The locked beat note at 2.9 GHz produced between SG-DBR and comb was connected to the ESA and the single-sideband (SSB) phase-noise spectral density (PNSD) was then measured. The signal power level of this measurement was 42 dBm. Figure 11 shows the residual OPLL phase noise at offsets from 10 Hz to 1 GHz. For the comparison, PNSD of the background, RF synthesizer at 2.9 GHz, and comb source (through the RF beat note generated between comb lines) are superimposed in Fig. 11. The output signal power levels were kept the same during the measurement in order to obtain consistency.

Optics EXPRESS

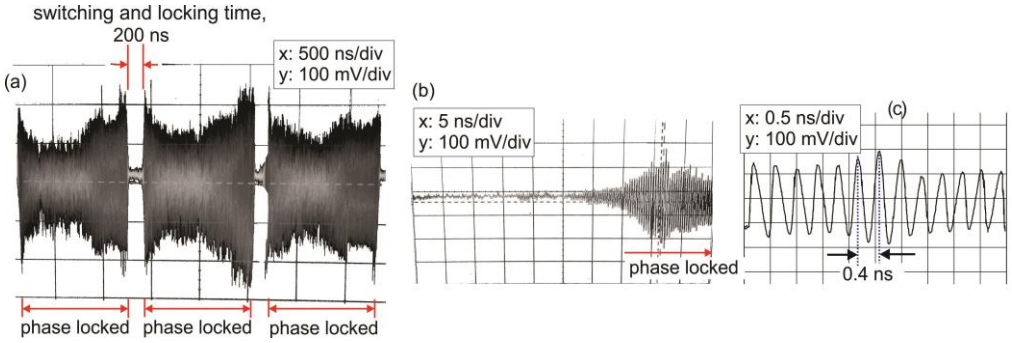

Fig. 10. (a) A real-time oscilloscope trace of the external photodiode output of both wavelength component of SG-DBR laser during wavelength switching in order to measure the locking time of the OPLL system. Three periods are shown here which corresponds to the modulation frequency of front mirror, i.e. 800 kHz, (b) trace with a smaller span, showing the transition to phase-locking, and (c) trace with smallest span to show 2.5 GHz signal during phase-locking.

The phase noise variance from 1 kHz to 10 GHz is calculated to be 0.08 rad^2, corresponding to 14° standard deviation from the locking point. This result is better than the one reported in [39]. As can be seen in Fig. 11, low frequency noise with a value less than 80 dBc/Hz at an offset above 200 Hz for PNSD was achieved., whereas the same value at an offset above 10 kHz was achieved in [29, 42]. Lu et al. also reported better than 80 dBc/Hz at offsets above 5 kHz which is again worse than the performance reported here [35]. However, the phase variance of our results is comparable with [29, 42] which could be attributed to the pedestal after 1 kHz which may be caused by a fiber path length mismatch between the comb and OPLL laser paths (see Fig. 5). Thus, after 1 kHz some additional noise from the slave laser is observed and contributes to the overall phase variance. Matched path length will be used in the future work.

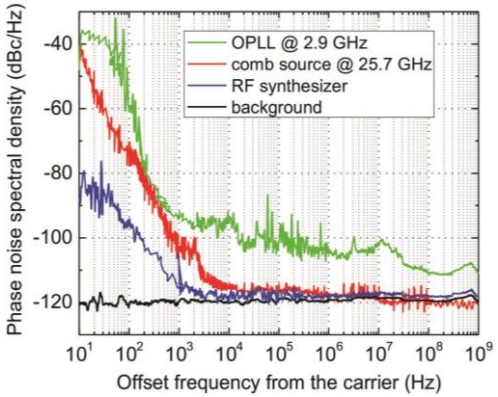

Fig. 11. Single-sideband residual phase noise of the heterodyne OPLL at 2.9 GHz. Phase noise results of the RF signal at 25.7 GHz generated between comb lines, RF synthesizer, and background is also shown here for comparison.

6. Summary and outlook

In this work, a chip-scale optical frequency synthesis spanning 25 nm is demonstrated. A stable heterogeneously integrated Kerr frequency comb characterized with 26 GHz repetition rate is used as a reference. Better than 100 Hz resolution within an accuracy of 5 Hz, which is the highest resolution reported for chip-scale optical frequency synthesis, is obtained. Both switching between two adjacent comb lines as well as multiple comb lines (i.e. 28 lines) separated by 5.6 nm and phase locking at the same time are achieved. As a future work, our

Optics EXPRESS

main goal is to develop a fully chip scale synthesizer which requires to replace the EDFA used in this study with on-chip SOAs. Instead of amplifying the power in the optical domain, we can increase the sensitivity of our electronic ICs as an alternative so that the weak error signal generated by beating on-chip laser and low-power comb line at the balanced photodiodes can be handled by the feedback electronics. Specifically, the sensitivity of our OPLL system can be increased by using ultrahigh-gain amplifiers with low noise figure or designing an application specific IC so that on-chip lasers can be phase locked to a comb line without an EDFA. This will open a new era for optical communications and sensing. This work will allow OPLL systems to be as useful as traditional RF phase-locked loops. In addition to this, another important goal is to achieve a 2/3 octave spanning optical frequency comb and use this as a reference source. This will allow us to have a broader synthesizer.

Funding

This work was supported by the GOALI project funded by the National Science Foundation (NSF) under Grant No. 1402935.

Acknowledgment

A portion of this work was carried out in the UCSB nanofabrication facility, part of the NSF funded NNIN network.